RSC Advances

PAPER

View Article Online
View Journal | View Issue

Cite this: *RSC Adv.*, 2025, **15**, 38044

Quantitative proteomic and glycoproteomic analysis identifies CLCA1, FBN1, and FGB as potential biomarkers for ulcerative colitis

Xiaotong Wang,†[acd] Siyue Bo,†[c] Qinkai Li,†[d] Wentong Li,[e] Longjiang Xu,[e] Duanmin Hu*[d] and Shuang Yang *[bcd]

Ulcerative colitis (UC), a prevalent inflammatory bowel disease (IBD), significantly increases the risk of colorectal cancer with prolonged duration. Current diagnostic approaches for UC rely on clinical symptoms, inflammatory markers, and endoscopic findings. However, these methods often face challenges due to symptom overlap with Crohn's disease (CD) and other gastrointestinal conditions. This highlights a critical need for reliable biomarkers in human body fluids for accurate UC diagnosis and effective therapeutic intervention. To address this, we employed quantitative proteomic and glycoproteomic analysis using liquid chromatography-mass spectrometry on proteins extracted from UC tissues and paracancerous (PCA) tissues. Our comprehensive findings revealed that three differentially expressed glycoproteins (CLCA1, FBN1, and FGB) are likely associated with UC, although their expression patterns differ slightly different from those in CD. Site-specific glycosylation analysis further revealed that each *N*-glycosylation site contained distinct *N*-glycans, and their fold changes are similar to the overall protein changes. We validated both the protein and gene expression of these glycoproteins through immunohistochemistry and RT-qPCR. Gene Ontology and Kyoto Encyclopedia of Genes and Genomes analyses indicated a possible functional correlation of CLCA1 with endopeptidase activity and FGB with the collagen-containing extracellular matrix. Furthermore, enzyme-linked immunosorbent assay (ELISA) quantification of these glycoproteins in the serum of UC and CD patients showed increased expression of FGB and reduced expression of CLCA1 in both conditions, while FBN1 levels remained unchanged. These results collectively suggest that the quantitative analysis of site-specific glycosylation profiles could be crucial for differentiating UC from CD, thereby facilitating earlier and more accurate diagnosis.

Received 20th July 2025
Accepted 6th October 2025

DOI: 10.1039/d5ra05241f

rsc.li/rsc-advances

Introduction

Ulcerative colitis (UC) is a chronic and remitting inflammatory bowel disease (IBD) that primarily affects the colon and rectum.[1] The clinical presentation of UC is highly variable, ranging from mild, non-specific symptoms to severe manifestations such as hematochezia, persistent diarrhea, fecal urgency, tenesmus, and abdominal cramping.[2] Beyond gastrointestinal symptoms, approximately 25 to 40% of UC patients experience extra-intestinal manifestations (EIM), which can sometimes precede the onset of gastrointestinal involvement.[3] The unpredictable course and chronic nature of UC significantly impact patient quality of life, necessitating continuous monitoring and management. Thus, reliable biomarkers are crucial for early diagnosis of UC and for prognosticating treatment effectiveness.[4]

Current diagnostic approaches for IBD integrate clinical assessment, laboratory tests, radiological imaging, and critically, endoscopy with biopsy and histological analysis. Endoscopy remains the gold standard, offering direct visualization of mucosal inflammation and tissue acquisition for definitive diagnosis and disease activity assessment. Routine blood and stool tests, such as fecal calprotectin (FCP), are widely used to assess inflammation. FCP, a neutrophil-derived protein, is often elevated in IBD patients,[5] offering greater specificity for colonic inflammation and correlating well with mucosal healing in both UC and CD. Its upregulation also aligns with gut microbial dysbiosis and serum inflammation.[6] However, endoscopy is invasive, expensive, and carries inherent risks like perforation or bleeding, limiting its frequent use for routine monitoring.

[a]*Department of Hepatology and Gastroenterology, The Affiliated Infectious Hospital of Soochow University, Suzhou 215004, China*

[b]*Laboratory of Clinical and Molecular Glycobiology, Institute of Glycomics, The First Affiliated Hospital of Shantou University Medical College, Shantou, Guangdong 515041, China. E-mail: shuangyang@stu.edu.cn*

[c]*Center for Clinical Mass Spectrometry, School of Pharmaceutical Sciences, Soochow University, Suzhou 215123, China*

[d]*Department of Gastroenterology, The Second Affiliated Hospital of Soochow University, Suzhou, Jiangsu 215004, China. E-mail: huduanmin@163.com*

[e]*Department of Pathology, The Second Affiliated Hospital of Soochow University, Suzhou, Jiangsu 215004, China*

† These authors contribute equally to this work.

Moreover, existing non-invasive biomarkers have significant limitations. While useful, FCP lacks specificity for a definitive IBD diagnosis, as its elevated levels can also indicate infections or even colorectal cancer.[7,8] C-reactive protein (CRP), a simple blood test, measures non-specific inflammation,[9] and aids in assessing cardiovascular diseases (CVD).[10] Similarly, CRP lacks specificity because various inflammatory conditions, not exclusively IBD, can elevate its CRP levels. Notably, CRP is less sensitive in UC than in CD, often showing only a modest or absent response even in patients with active UC.[11]

The diagnosis of UC is complicated by its heavy reliance on invasive procedures and the limitations of current non-invasive biomarkers like FCP and CRP. These biomarkers often lack specificity or present practical challenges, leading to delayed or inaccurate diagnoses and suboptimal treatment. Ultimately, this significantly negatively impacts patient quality of life. Therefore, there's an urgent need for novel, highly specific, and less invasive diagnostic and monitoring tools for UC. Improved biomarkers are crucial to accurately differentiate UC from conditions such as irritable bowel syndrome (IBS)[12] or acute gastroenteritis (AGE),[13] identify patients at high risk for severe disease progression, complications, or relapse, and guide personalized treatment strategies by predicting individual responses to specific drugs. Given the strong association between disease states and post-translational modifications (PTMs),[14] with abnormal glycosylation often reflecting pathophysiological status,[15] investigating disease-specific glycosylation (DSG) holds promise for significantly enhancing biomarker specificity and sensitivity.[16–18] Therefore, studying glycosylation in UC is vital for developing reliable biomarkers that can assess disease activity and mucosal healing without repeated invasive endoscopic procedures, and facilitate the discovery of UC molecular subtypes for more targeted and effective interventions.[19,20]

Glycosylation alterations are implicated in various diseases. In UC, genetic disruptions in *O*-glycan biosynthesis lead to truncated *O*-glycans of MUC2 mucin, frequently forming dense *N*-acetylgalactosamine (Tn) and galactose-*N*-acetylgalactosamine (T) antigens.[21] These shorter *O*-glycans on mucosal mucins compromise the colon's protective barrier against bacteria, enzymes, and chemicals, as mucin *O*-glycans typically facilitate symbiosis to maintain gut immune homeostasis and act as a physical protective layer.[19] Dysregulation of glycoenzymes (glycosyltransferases and glycosidases) also contributes to altered glycosylation in disease.[22] For instance, elevated levels of sialic acid *O*-acetylesterase (SIAE) in UC lead to reduced acetylation of sialic acids, which are subsequently hydrolyzed by sialidases (neuraminidase, NEU1), resulting in decreased cell surface sialic acid expression and impaired cell–cell adhesion.[23] Comprehensive pathway analyses indicate that innate microbial sensing, adaptive immunity, cytokine networks, and epithelial barrier function are crucial in UC risk.[24,25] Furthermore, oncogene protein glycosylation, induced by pathways like endoplasmic reticulum (ER) stress, can alter the biological functions of immune macrophage inflammatory proteins, thereby advancing the pathogenesis of UC and even colitis-associated cancer (CAC).[4,26,27] However, the precise mechanisms by which these pathway alterations affect protein glycosylation in pathological tissue and serum remain to be elucidated.

This study aimed to identify glycoprotein biomarkers for UC diagnosis using a comprehensive mass spectrometry-based approach (Fig. 1). Tissue samples, specifically paracancerous (PCA) and UC tissues, underwent homogenization and protein extraction. These proteins were then subjected to tryptic digestion to yield peptides. Ten percent of these peptides were analyzed for global protein expression using C18 chromatography, while the remaining peptides were enriched for glycoproteins *via* hydrophilic interaction liquid chromatography (HILIC) for glycoproteomic analysis. Both global and glyco-enriched peptide samples were then analyzed by bottom-up liquid chromatography-tandem mass spectrometry (LC-MS/MS) to generate MS spectra for label-free quantitative analysis. In parallel, serum samples from UC patients, CD patients, and healthy controls (HC) were analyzed for the expression levels of specific glycoprotein candidates (CLCA1, FBN1, and FGB), using ELISA (Enzyme-linked immunosorbent assay) for validation and quantitative analysis. This multi-faceted approach, combining tissue proteomics and glycoproteomics with serum-based ELISA validation, seeks to identify and characterize novel glycoprotein biomarkers for UC diagnosis.

Materials and methods

Clinical sample collection

Clinical UC and PCA tissues were obtained from patients undergoing colectomy or diagnostic endoscopy. For this study, a diverse range of samples was used for different analytical techniques to ensure a comprehensive evaluation. Specifically, we collected three ulcerative colitis (UC) and three paracancerous tissue (PCA) samples for both global and glycoproteomics studies. For immunohistochemistry, we utilized tissue slides from 10 UC and 20 PCA patients to examine protein localization. Finally, for the enzyme-linked immunoassay (ELISA), we collected serum from three UC and three healthy control individuals to quantify protein levels. All clinical specimen collection procedures adhered to ethical guidelines and received approval from the Institutional Review Board of the Second Affiliated Hospital of Soochow University, with informed consent secured from all participants (JD-LK2023117-I01). Upon collection, tissue samples were immediately flash-frozen in liquid nitrogen and stored at −80 °C to preserve protein integrity and prevent degradation. Prior to protein extraction, frozen tissues were carefully weighed and prepared for homogenization.

Tissue protein extraction

Proteins were extracted from the homogenized UC and control colon mucosal tissues using a standardized protocol optimized for maximizing protein yield and minimizing degradation. Initially, tissue samples were thoroughly washed with ice-cold 1x PBS to eliminate blood and external contaminants, then gently dried in sterile, lint-free tube. Each dried tissue sample was precisely weighed using an analytical balance to a precision

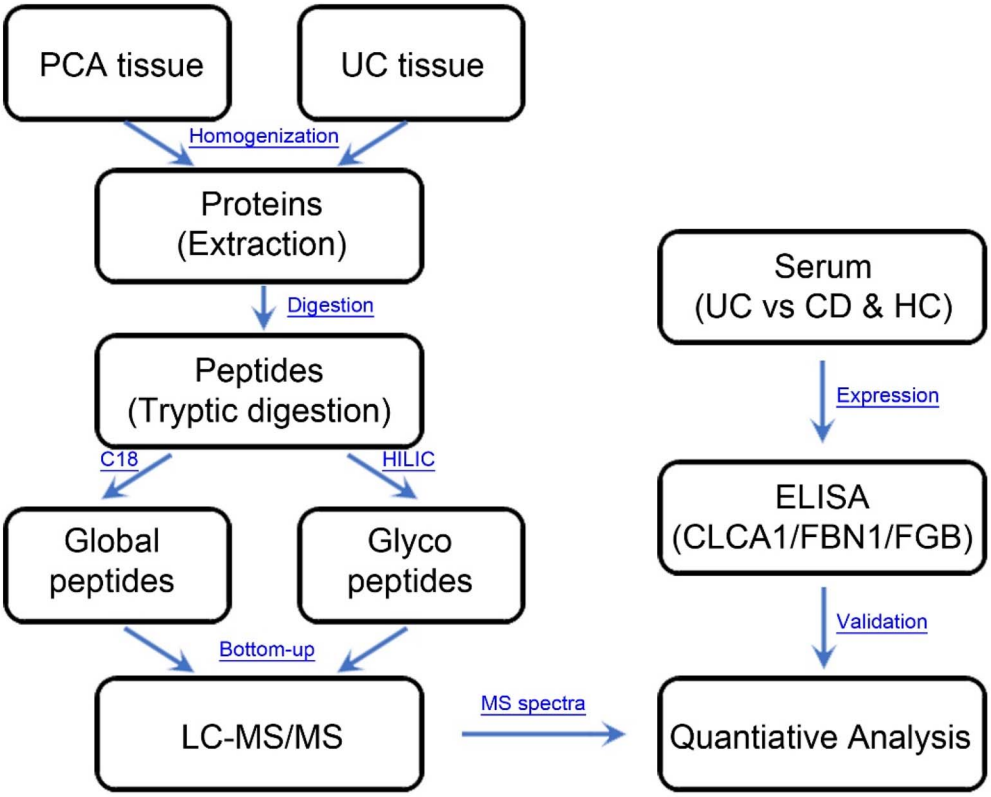

Fig. 1 Schematic diagram of glycoproteomic analysis of protein glycosylation in UC. Clinical specimens are collected, followed by protein extraction and tryptic digestion. Global peptides are purified using a C18 solid-phase extraction (SPE) cartridge, while glycopeptides are enriched *via* HILIC-SPE. Both fractions are then quantitatively analyzed by liquid chromatography-tandem mass spectrometry (LC-MS/MS). The potential glycoprotein markers are further verified using enzyme-linked immunoassay (ELISA).

of 0.1 mg. Subsequently, pre-chilled RIPA buffer, at a volume approximately ten times the tissue weight (*e.g.*, ~20 mg tissue received ~200 μL buffer), was added along with a 1x protease inhibitor. The tissue was then mechanically lysed using a handheld homogenizer until a uniform mixture was achieved. Following homogenization, the lysate was incubated on ice for 20–30 minutes with gentle vortexing every 5 minutes to enhance protein extraction. Finally, the lysate was centrifuged at 12 000×*g* for 15 minutes at 4 °C, and the protein-containing supernatant was carefully transferred to a new tube, avoiding disturbance of the pellet. The extracted proteins were then either stored on ice for immediate use or frozen at −80 °C for long-term preservation.

Protein tryptic digestion for global proteins and glycoproteins

For protein tryptic digestion and subsequent purification of peptides and intact glycopeptides, protein concentration was first determined by a BCA assay. Then, 2 mg of protein was denatured in 200 μL of 8 M urea (Aladdin, China) prepared in 1 M NH_4HCO_3, followed by reduction with 20 μL of 120 mM TCEP (Macklin, China) at 37 °C for 1 hour, and subsequent alkylation with 20 μL of 160 mM IAA (Aladdin, China) at room temperature for 1 hour in the dark. The alkylated samples were then diluted 5-fold with HPLC grade water (J&K, China) to reduce the urea concentration for overnight digestion at 37 °C with 40 μg of sequencing grade trypsin (Promega, US). Tryptic digestion was quenched by adjusting the pH to below 3 with 10% formic acid, and the resulting peptides were purified using C18 SPE (Silicycle, Canada) to remove contaminants. For glycopeptide enrichment, the C18-purified peptides were dissolved in 80% ACN with 0.1% TFA (Macklin, China) and loaded onto a HILIC-SPE column containing Amide-80 gel slurry (Tosoh, Japan), with the flow-through reloaded to maximize capture. The column was washed three times with 80% ACN in 0.1% TFA, then sequentially eluted with 60% ACN in 0.1% TFA, 40% ACN in 0.1% TFA, and 0.1% TFA to collect enriched glycopeptide fractions.[28] The pooled eluate, containing purified peptides and glycopeptides, was then dried in a vacuum concentrator prior to LC-MS/MS analysis.

LC-MS/MS analysis of peptides and glycopeptides

Both peptides and intact glycopeptides were separated and analyzed using an easy-nanoLC 1200 system coupled to a Q-Exactive HF-X Hybrid Quadrupole-Orbitrap Mass Spectrometer (Thermo Scientific). 1 μg of peptides or glycopeptides were injected and desalted on an Acclaim PepMap C18 Nano-Trap column (3 μm, 100 Å, 75 μm × 2 cm) at a flow rate of 5 μL min^{-1} with 100% solvent A (0.1% formic acid in HPLC water) for 5 minutes. The samples were then separated on an Acclaim PepMap 100 Nano-Column (3 μm, 100 Å, 75 μm × 250 mm)

using a linear gradient of 2.5–37.5% solvent B (80% ACN, 0.1% formic acid) over 85 minutes, followed by a 5 minute wash with 90% B. The column was equilibrated with 2.5% B for 10 minutes before the next injection. Data-dependent acquisition (DDA) with a duty cycle of 2 seconds was employed with a static spray voltage, static gas mode, and EASY-IC internal quality calibration. For primary mass spectrometry (MS1), a resolution of 120 000 was used with a scanning range (m/z) of 375–2000, an AGC target of 10^6, positive polarity, dynamic exclusion 20 seconds, and inclusion of charge states 2–8. The secondary mass spectrometry (MS2) had a resolution of 60 000, an ion selection window of 1.2, a first mass of 110, and a standardized AGC target of 250%. For intact glycopeptides, stepped higher-energy collisional dissociation (HCD) spectra were acquired at 15%, 25%, and 35% HCD energy for precursors with charges between 2–8 and intensities exceeding 5.0×10^4 at a resolution of 30 000, with dynamic exclusion set at 20 seconds. Acquisition of glycopeptide-specific MS2 spectra was triggered when at least one glycan oxonium fragment ion (m/z 138.0545, 204.0867, 366.1396 Da) was observed within the top 20 most abundant fragments and within 15 ppm mass accuracy.

Gene ontology and KEGG analysis

Differentially altered proteins, identified by their corresponding genes, were subjected to gene ontology (GO) and Kyoto Encyclopedia of Genes and Genomes (KEGG) analysis using ShinyGO 0.81 bioinformatics.[29] GO enrichment analysis served to classify these differentially expressed glycoproteins into functional categories, encompassing biological processes, molecular functions, and cellular components. Concurrently, KEGG analysis mapped these proteins onto molecular interaction, reaction, and relation networks, revealing pathways generally correlated with the development and progression of UC.

Validation of altered expression of glycoproteins in UC

To rigorously validate the findings from MS and bioinformatics analyses, the three differentially expressed glycoproteins identified as having strong UC specificity were further characterized using orthogonal experimental techniques: immunohistochemistry, RT-qPCR (primers are given in Table S1), and ELISA. This multi-level validation provides robust evidence of differential expression at both gene and protein levels and confirms their presence in circulating blood.

UC tissue immunohistochemistry

Human colon tissue paraffin sections were obtained from the Pathology Department of the Second Affiliated Hospital of Soochow University. All patients signed informed consent forms before sample collection. Among them, UC patients were diagnosed based on clinical manifestations, endoscopic examination, and histological standards ($n = 10$; 6 males and 4 females; aged 16–69 years). Control intestinal biopsy samples were taken from PCA tissues ($n = 20$; 12 males and 8 females; aged 45–72 years). After dewaxing the sections with xylene, they were treated with gradient ethanol (100%, 95%, 80%, 70%) and washed with PBS. Subsequently, antigen retrieval was performed by heating at 121 °C for 10 minutes in 10 mM citrate buffer (pH 6.0) under high pressure. To block endogenous peroxidase activity, sections were incubated in 3% hydrogen peroxide solution at room temperature for 10 minutes. After rinsing with 1xPBS, anti-CLCA1 antibody (rabbit; 1:200; Proteintech, Inc.; catalog no. 25291-1-AP), anti-FBN1 antibody (rabbit; 1:200; Proteintech, Inc.; catalog no. 29425-1-AP), and anti-FGB antibody (rabbit; 1:100; Proteintech, Inc.; catalog no. 16747-1-AP) were added respectively and incubated at room temperature for 2 hours. Subsequently, detection was performed using goat anti-rabbit HRP secondary antibody (Thermo Scientific, Inc.; catalog no. C31460100) and DAB (catalog no. 34065) for color development. Finally, sections were counterstained with hematoxylin, rinsed with running water, differentiated with hydrochloric acid ethanol, dehydrated, and mounted for observation and photography under a microscope.

Validation of serum glycoprotein expression by ELISA

ELISA was used to detect the content of target proteins in serum samples from UC, CD, and HC. Before the experiment, the kit (Shanghai Enzyme-linked Biotechnology) was taken out of the 4 °C refrigerator and allowed to equilibrate at room temperature for 20 minutes, and the serum samples to be tested were kept on ice. Standards were prepared according to the kit instructions, and a standard curve was established (replicates for each concentration), along with blank and sample wells. 50 μL of gradient concentration standards were added to the standard wells, and 50 μL of serum to be tested was added to the sample wells. Except for the blank wells, 100 μL of HRP-labeled detection antibody was added to each well. After sealing with film, the plate was incubated at 37 °C for 60 minutes. After incubation, the liquid was discarded and blotted dry. 350 μL of wash buffer was added to each well, left for 1 minute, and then shaken dry; this washing step was repeated 5 times. Subsequently, 50 μL of substrate A and B were added sequentially to each well, and color was developed at 37 °C in the dark for 15 minutes. Finally, 50 μL of stop solution was added to quench the reaction, and the OD value was measured at 450 nm within 15 minutes using an ELISA reader. A standard curve was plotted using Excel with standard concentrations on the x-axis and OD values on the y-axis, and the concentration of each sample was calculated based on the regression equation.

Results and discussion

Differentially regulated proteins in UC

In this study, a comprehensive proteomics approach was employed to analyze proteins extracted from the tissues of three UC patients and three PCA patients. Following trypsin digestion and C18 desalting, LC-MS/MS analysis was performed, revealing over 462 differentially regulated proteins between UC and PCA (Table S2). A volcano plot (Fig. 2), comparing UC and PCA, distinctly illustrates that 9 proteins were significantly upregulated (fold-change > 1.5, p-value < 0.05) (These criteria indicate a substantial and statistically significant increase), while another 9 proteins were significantly downregulated (fold-

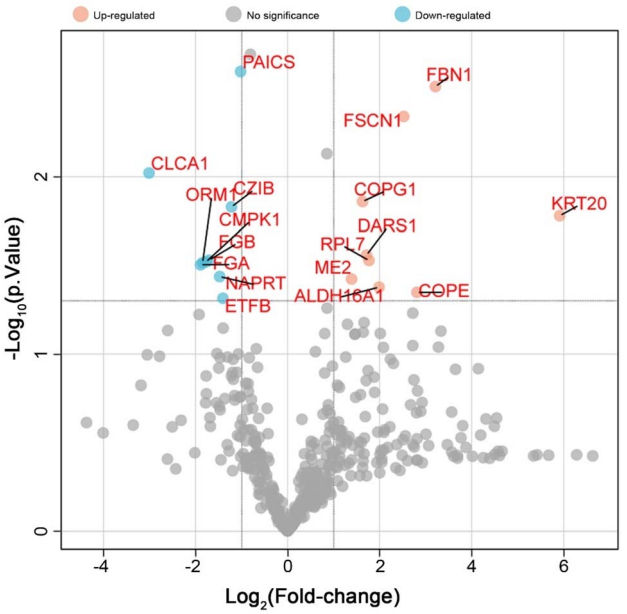

Fig. 2 The volcano plot illustrating the differentially expressed proteins between UC and PCA tissues, derived from the analysis of three UC and three PCA patient samples. The *x*-axis represents the fold-change (FC) between UC and PCA, while the *y*-axis represents the negative logarithm (base 10) of the *p*-value. Statistical significance was determined using Student's *t*-test, with a *p*-value less than 0.05 indicating a statistically significant difference.

change < 0.67, *p*-value < 0.05) (These criteria indicate a substantial and statistically significant decrease). Notably, among the upregulated proteins, KRT20 showed a substantial 5.9-fold increase in UC, followed by FBN1 (3.2-fold), COPE (2.8-fold), FSCN1 (2.5-fold), ALDH16A1, RPL7, DARS1, COPG1, ME2, and SNRPD3. Conversely, CLCA1, FGA, ORM1, CMPK1, FGB, NAPRT, ETFB, CZIB, PAICS, and STRAP were significantly decreased in UC. These results suggest that altered protein expression may be associated with inflammation pathogenesis.

Protein glycosylation altered in UC compared to PCA

Intact glycopeptides were identified and analyzed using MSFragger and Byonic. Site-specific intact glycopeptides found in both UC and PCA tissues are presented in Fig. S1 and Table S3, with their relative abundances visualized in a violin plot. A notable finding was the decreased *N*-glycosylation of MUC2 in the mucosal layer, which aligns with expectations since reduced *N*-glycosylation diminishes the protective function of mucus; indeed, studies have shown that UC can lead to a 60% decrease in Muc2 levels and complex glycans.[30] However, truncated *O*-glycans weren't found in this study. The identification of protein *O*-glycosylation requires different analytical methods, specifically the use of *O*-glycoproteases and alternative mass spectrometric detection techniques like electron transfer dissociation (ETD). This work used HILIC to enrich tryptic peptides and relied on higher-energy collision dissociation (HCD), which isn't suitable for detecting MUC2 *O*-glycopeptides. These glycoproteins collectively contribute to diverse cellular functions: DCN, LAMC1, LUM, and MUC2 are extracellular matrix and structural components whose altered glycosylation can significantly impact cell adhesion, differentiation, and signaling.[31] HPX and HP function as transport and binding proteins, potentially safeguarding cells from oxidative damage, while ITGA1 acts as a cell-surface receptor for collagen and laminin, playing a role in regulating inflammatory response.[32] Furthermore, several identified glycoproteins are enzymes with various catalytic activities; for instance, CTSA is a protease that degrades other proteins, and its aberrant glycosylation is frequently associated with cancer and inflammation.[33] CTSL is another thiol protease crucial for protein degradation, and POGLUT3 that catalyzes the *O*-glucosylation of proteins was correlated to inflammation *via* notch signaling.[34,35] Importantly, HSP90B1, SSR2, and STT3A/STT3B are vital molecular chaperones and protein processing enzymes, with alterations in STT3A/STT3B directly leading to altered *N*-glycosylation of proteins.[36]

Among the glycoproteins identified in Fig. S1 and Table S3, significantly altered glycosylation sites are elaborated in Fig. 3. Specifically, the CTSA glycopeptide, MDPPCTN[327]TTAASTYLNNPYVR, exhibited a significantly elevated H5N3 glycan in UC compared to PCA, as shown by relative abundance in the violin plot. Similarly, the HPX glycopeptide, ALPQPQN[454]VTSLLGCTH, displayed a decreased relative abundance of the S2H5N4 glycan at N454 in UC. The LUM glycoprotein showed an elevated S1H5N4F1 glycan at glycosite N127. Interestingly, STT3A carried one glycosite, but was associated with two distinct *N*-glycans: H8N2 and H9N2. Additionally, the TPP1 glycopeptide, FLSSSPHLPPSSYFN[438]ASGR, featured a fucosylated *N*-glycan (H3N2F1) that was upregulated in UC. These findings collectively suggest that site-specific quantitative glycopeptide analysis holds promise for differentiating UC from PCA.

We further examined the glycoforms of several key glycoproteins. Fig. 4 illustrates the annotation of MS2 fragments of intact glycopeptides from CLCA1 and FGB. While the fragmentation ions were almost identical between PCA and UC, we observed subtle differences in fucosylation. Specifically, the CLCA1 peptide (ASNATLPPITVTSK) from PCA contained S1H5N4F2, whereas the corresponding peptide in UC had S1H5N4F1, suggesting reduced fucosylation in UC. Conversely, the FGB peptide (GTAGNALMDGASQLMGENR) exhibited higher fucosylation in UC, with two fucose residues compared to none in PCA. These findings demonstrate that even subtle changes in site-specific glycosylation can occur in different pathophysiological states.

UC-specific glycosylation in triple glycoproteins

To identify glycoproteins associated with UC, we investigated three candidate proteins: CLCA1, FBN1, and FGB. We performed immunohistochemistry (IHC) staining on tissue samples from both UC and PCA, using monoclonal antibodies specific to each glycoprotein. As depicted in Fig. 5A, the mucosal layer in UC tissues appeared damaged when compared to PCA tissues. Furthermore, IHC staining revealed a decrease

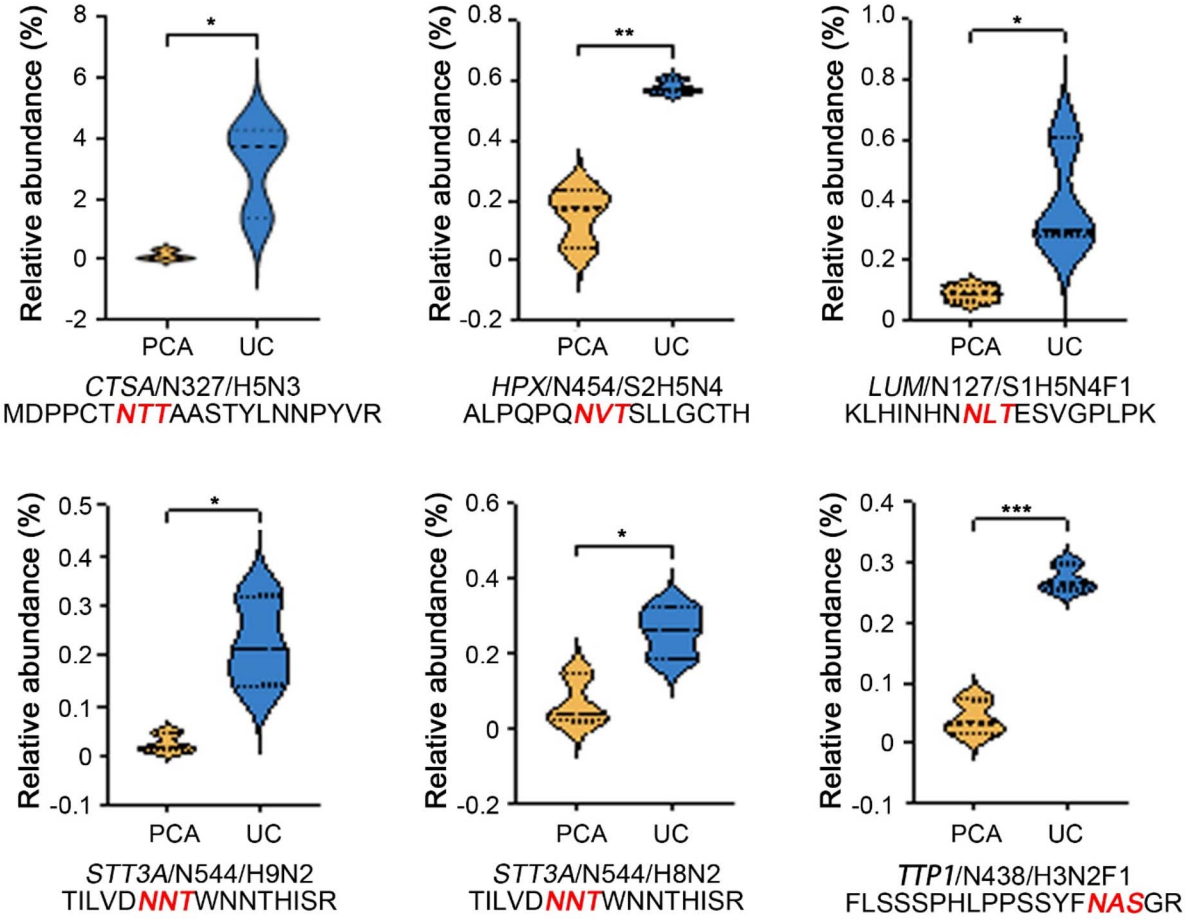

Fig. 3 Altered protein glycosylation between UC and PCA. The relative abundance of five glycoproteins shows significant differences in glycosylation between UC (blue) and PCA (orange) tissue specimens. The violin plots illustrate the distribution of intact glycopeptides identified for each protein. Specifically, the plots show the relative abundance of CTSA (with glycan composition H5N3 at *N*-glycosite 327), HPX (S2H5N4), LUM (S1H5N4F1), STT3A (H9N2 and H8N2), and TTP1 (H3N2F1). The specific amino acid sequence containing the glycosylation motif is shown below each plot, with the glycosylation site highlighted in red. Statistical significance was determined using an unpaired Student's *t*-test, with *p*-values indicated as follows: $*p < 0.05$, $**p < 0.01$, and $***p < 0.001$. Glycan abbreviations are as follows: H = Hexose, N = HexNAc, S = Neu5Ac, F = Fucose.

in protein expression of CLCA1 and FGB in UC samples, while FBN1 protein expression was notably elevated in UC, consistent with the quantitative analysis of protein expression shown in Fig. 5A. Subsequent RT-qPCR quantification of gene expression levels showed a similar trend to the protein expression data; however, these analyses do not directly provide insights into potential glycosylation alterations in UC.

The quantitative characterization of protein glycosylation can be effectively achieved through bottom-up glycoproteomics, a technique where tryptic peptides undergo HILIC-SPE enrichment for intact glycopeptides.[37,38] Given its exceptional hydrophilic and polar interactions due to non-ionic carbamoyl groups, Amide-80 has been widely employed for the enrichment of intact *N*-glycopeptides.[28,39] Fig. 5B illustrates the site-specific glycosylation profiles of the target glycoproteins using MSFragger and Byonic search, in which FDR is set to be 1% and PEP2D (posterior error probability 2D) less than 0.5. In this representation, glycosites are denoted by a three-letter code where 'N' signifies asparagine, 'S' for serine, and 'T' for threonine, with the second letter representing any amino acid except proline. The glycan compositions are indicated by 'N' for HexNAc, 'H' for Hexose, 'F' for Fucose, and 'S' for Neu5Ac. The "FC (Global)" and "FC (Glyco)" values represent the fold-change of global protein and glycoprotein expression, respectively, in UC compared to PCA. Specifically, CLCA1 N[585]AT exhibited high fucosylation and an increased number of *N*-glycans in UC, while no *N*-glycans were detected at N[503]GT in UC. FBN1 at N[448]VT, N[1067]CT, and N[1581]TS showed similar glycosylation trends in UC relative to PCA. Interestingly, S2H5N4 was exclusively identified at N[394]AL of FGB in PCA. The observation that the FC in global protein expression was similar to that of glycopeptide expression suggests a possible correlation where protein upregulation or downregulation is accompanied by corresponding changes in its glycosylation.

KEGG-GO analysis on glycoproteins

Glycoproteins exhibiting altered expression in UC were further analyzed through GO and KEGG pathway enrichment to

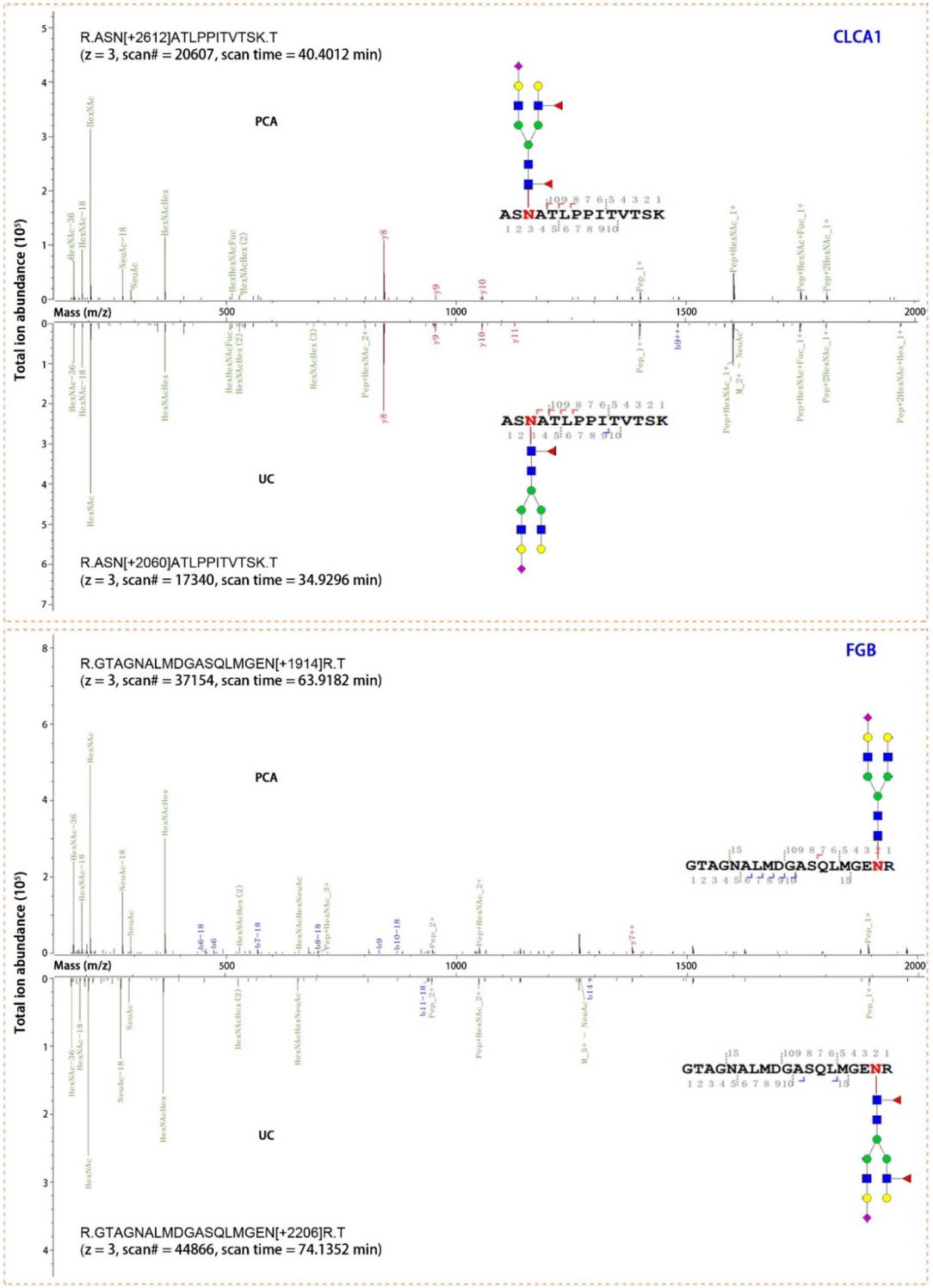

Fig. 4 Differential *N*-glycosylation patterns of CLCA1 and FGB in colon epithelial tissues from UC and PCA. The top two panels display the mass spectrometry (MS) annotation for the CLCA1 glycopeptide. In the PCA sample, the CLCA1 glycopeptide (ASN[S1H5N4F2]ATLPPITVTSK) elutes at 40.4 min. Conversely, in the UC sample, the CLCA1 glycopeptide (ASN[S1H5N4F1]ATLPPITVTSK.T) elutes earlier at 34.9 min. This indicates a difference in fucosylation and retention time for CLCA1 between PCA and UC. The bottom two panels show the MS annotation for the FGB glycopeptide. The UC sample shows that the FGB glycopeptide (GTAGNALMDGASQLMGEN[S1H5N4F2]R) elutes at 74.1 min and has two fucoses. In contrast, the PCA sample for FGB (GTAGNALMDGASQLMGEN[+1914]R) exhibits no fucosylation, as depicted by the glycan structure lacking fucose. These site-specific *N*-glycosylation analyses of CLCA1 and FGB demonstrate significant alterations in protein fucosylation patterns in UC compared to PCA.

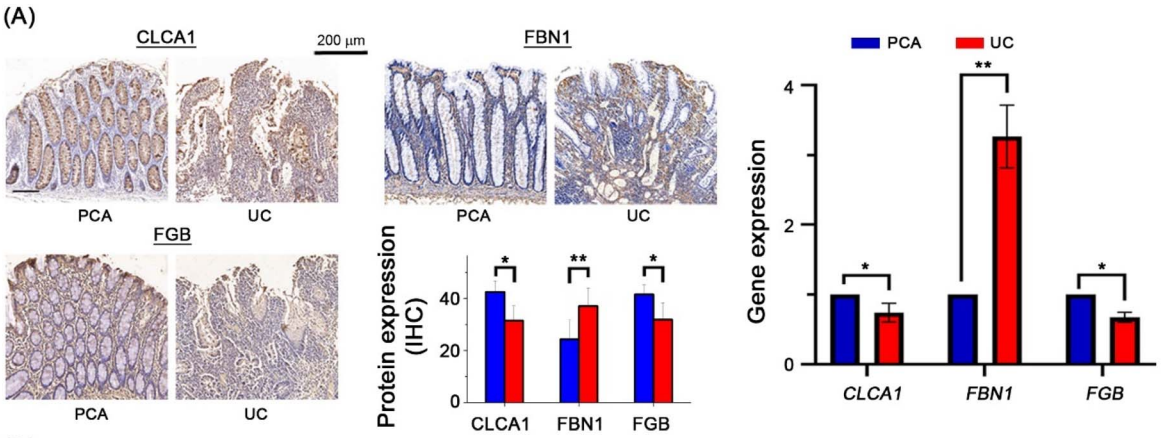

(B)

Gene	Protein	Glycosite	FC (Global)	Site-specific glycan profile		FC (Glyco)
				UC	PCA	
CLCA1	Calcium-activated chloride channel regulator 1	*N*[503]GT	0.12	/	H3N5F1/H4N5F1/H3N6F2	/
		N[585]AT		H4N5F2/H4N5F3/H5N4F3/H5N5F1 H5N5F2/H5N5F3/S1H5N5F1/H6N5F3 H6N5F4	H4N3F2/H3N4F3/H4N5F2 H4N4F3/H5N5F3	1.11
FBN1	Fibrillin-1	*N*[770]LT	9.27	H5N3F1/H6N3F1/H6N4F2	H5N3F1/H5N3F2/H6N3F1	0.72
		N[448]VT		S1H5N4F1	/	/
		N[1067]CT		H5N2/H6N2/H7N2/H4N4F2	H5N2/H6N2/H7N2	5.12
		N[1581]TS		H4N4F2	/	/
FGB	Fibrinogen β-chain	*N*[394]AL	0.30	H5N4/S1H5N4	S1H5N4/S2H5N4	0.39

Fig. 5 Differential expression and *N*-glycosylation profiles of key glycoproteins in UC compared to PCA. (A) The IHC data demonstrated that CLCA1 and FGB protein expression is downregulated in UC, while FBN1 expression is significantly increased in UC. Consistent with these findings ($n_{UC} = 10$ and $n_{PCA} = 20$ for IHC, $n_{UC} = 3$ and $n_{PCA} = 3$ for RT-qPCR). (B) Proteomic and glycoproteomic analysis showed CLCA1 and FGB significantly downregulated in UC, while FBN1 is upregulated. Furthermore, site-specific glycoproteomic analysis reveals that FBN1 is particularly elevated at the N[1067]CT glycosite in UC, with some glycosylation sites, such as N[448]VT and N[1581]TS, uniquely present only in UC. Overall, the glycosylation level on CLCA1 and FGB is observed to be reduced in UC.

elucidate their functional implications and potential correlation with disease pathogenesis (Fig. 6 & Table S4). As shown in Fig. 6B, significantly enriched biological processes include the integrin-mediated signaling pathway (IMSP), lysosome organization (LYO), and lytic vacuole organization (LVO). These pathways are critical to cellular adhesion, degradation, and waste management, all of which are frequently dysregulated in inflammatory conditions like UC. Furthermore, enriched cellular components such as vacuolar lumen (VAL), secretory granule lumen (SGL), and lysosomal lumen (LYL) suggest widespread disruption in intracellular vesicular trafficking and organelle function, indicative of cellular stress and altered homeostasis in the inflamed gut. At the molecular level, prominent functions identified include endopeptidase activity (EPA), serine-type exopeptidase activity (SEA), and extracellular matrix binding (EMB). These indicate a possible imbalance in protein degradation and tissue remodeling, processes crucial for maintaining the integrity of the intestinal barrier.

Fig. 6C further illustrates the significantly impacted KEGG pathways, with ECM-receptor interaction (ECMRI) and complement and coagulation cascades (CCC) demonstrating high statistical significance. These pathways are central to immune response, tissue integrity, and inflammatory processes, probably correlating the observed glycoprotein changes to the underlying pathogenesis of UC. These interactions between altered glycoproteins and various molecular functions, as presented in Fig. 6A, provide further insights; for example, CLCA1 interacts with serine-type peptidase activity (SPA) and serine hydrolase activity (SHA), while FGB interacts with collagen binding (COB) and phosphatase binding (PHB). The alterations in glycosylation patterns of CLCA1, FGB, and FBN1, coupled with their involvement in these critical GO terms and KEGG pathways, suggest their potential as specific biomarkers for UC. These glycoproteins, through their modified glycosylation, might reflect the ongoing extracellular matrix remodeling, immune dysregulation, and altered cellular degradation pathways characteristic of UC, making them promising candidates for diagnostic or prognostic indicators.

Validation of expression of glycoproteins in circulating blood

To validate the alterations of these glycoproteins in UC, we performed ELISA on serum samples from three HCs, three UC patients, and three CD patients, the latter serving as a positive control. Based on initial tests, a 20× dilution was used for ELISA

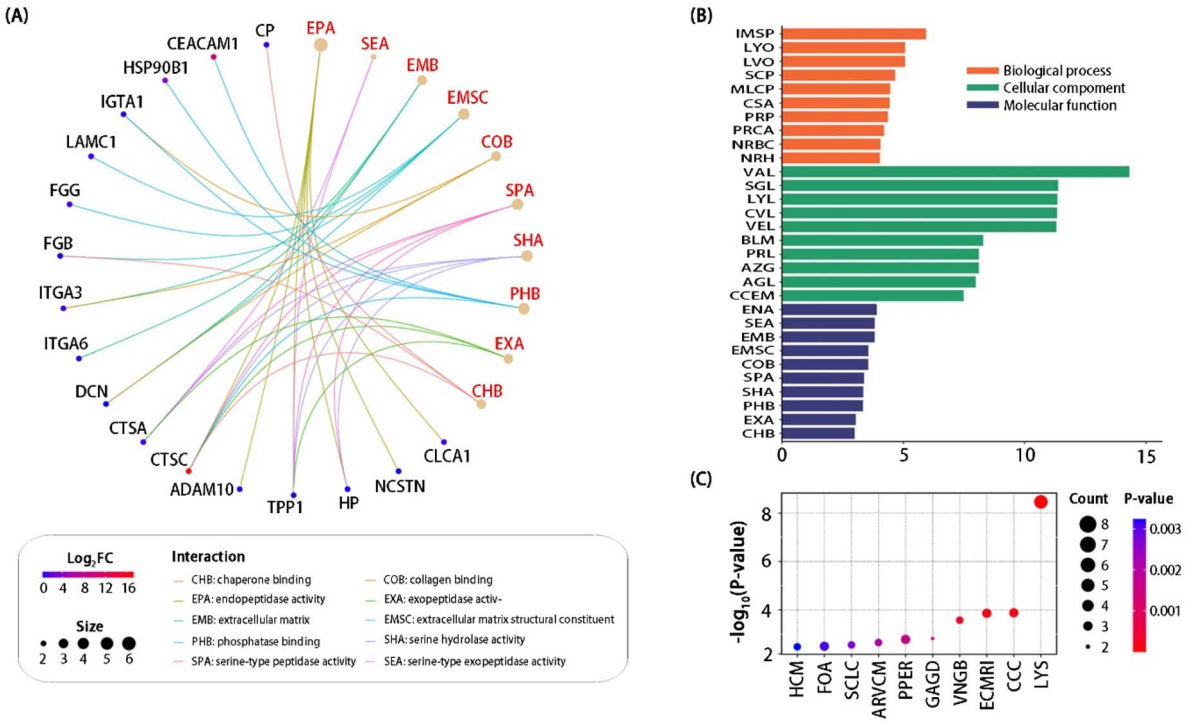

Fig. 6 Integrated gene ontology (GO) and KEGG pathway analysis of dysregulated glycoproteins in ulcerative colitis (UC). (A) A molecular function network visualization illustrated the relationships between dysregulated glycoproteins identified in UC (blue nodes) and their associated enriched GO molecular functions (beige nodes). The color intensity of the protein nodes indicates the Log_2(fold change) (Log_2FC) of their expression, ranging from low (purple) to high (red), signifying the extent of dysregulation in UC. The size of the protein nodes corresponds to the number of interactions or connections within the network, reflecting their centrality or involvement in multiple processes. The GO terms include a diverse biological activity. (B) A bar graph of GO analysis categorized the regulated protein glycosylation into top enriched biological processes and molecular functions, providing a quantitative overview of altered pathways. (C) KEGG pathway analysis showed specific pathways involved in the pathogenesis of UC that are impacted by these dysregulated glycoproteins, with dot size representing the count and color indicating the *P*-value.

measurements. Specifically, 2.5 μL of serum was mixed with 47.5 μL of dilution buffer from the respective ELISA kits (FGB: ml592612-1; CLCA1: ml060692-1; FBN1: ml105508-1). Each diluted sample (2.5 μL serum + 47.5 μL dilution buffer) was then added to 100 μL of HRP-labeled monoclonal antibody. As shown in Table 1, which presents the mean protein concentrations in serum from HC, UC, and CD individuals based on nine ELISA measurements (3 specimens × 3 technical replicates) with calculated standard deviations and *p*-values, distinct patterns emerged. CLCA1 concentration was found to be higher in the serum of HC individuals but lower in both UC and CD patients. Interestingly, despite FBN1 exhibiting altered glycosylation in UC in our prior MS analysis, its serum concentration showed negligible changes in UC or CD compared to HC. In contrast, we observed a significantly increased concentration of FGB in both UC and CD serum, with 4.34-fold and 2.70-fold changes, respectively, relative to HC. These results might suggest that while serum FGB concentration could serve as a biomarker to differentiate IBD patients (UC and CD) from HCs, the unique glycosylation patterns of these glycoproteins, particularly FBN1 and CLCA1, might potentially allow for the differentiation between UC and CD. The observation of increased FGB levels in

Table 1 Concentration of three glycoproteins in serum, measured by enzyme-linked immunosorbent assay (ELISA). Healthy controls (HC) are individuals without ulcerative colitis (UC) or Crohn's disease (CD). All serum samples were diluted 20x using 1x PBS buffer, and each sample was measured in triplicate. STD indicates standard deviation; FC represents fold-change. The *P*-value was calculated using a Student's *t*-test based on nine experiments, which consisted of three individual specimens with three technical replicates each

	HC (μg mL^{-1})		UC (μg mL^{-1})				CD (μg mL^{-1})			
Glycoprotein	Mean	STD (±)	UC	STD (±)	FC	*p*-Value	CD	STD (±)	FC	*p*-Value
FGB	15.1	0.43	65.55	3.1	4.34	0.0056	40.82	4.73	2.70	0.0052
FBN1	83.2	7.84	85.51	8.12	1.03	0.097	92.97	12.67	1.12	0.115
CLCA1	105.32	16.09	45.04	4.87	0.43	0.018	32.39	4.80	0.31	0.004

the serum but decreased levels in the colon is not a contradiction; rather, it may highlight distinct biological processes. FGB is an acute-phase reactant protein whose production by the liver is stimulated by inflammatory cytokines, such as IL-6.[40] This systemic, liver-driven response may lead to a significant increase in serum FGB, which accounts for the elevated levels in the bloodstream. Conversely, the lower FGB concentration in the inflamed colon tissue likely reflects local factors, including the continuous consumption of the protein for wound healing and clotting at the site of tissue damage due to vascular leakage and matrix remodeling.[41] Our future work will focus on comprehensively studying the glycoforms of these glycoproteins in both tissue and serum samples from UC and CD patients to further solidify their roles as UC-specific biomarkers.

Challenges and limitations of the study

This study, while providing compelling evidence for novel glycoprotein biomarkers in UC, acknowledges several significant challenges and limitations. The small sample sizes and lack of mechanistic data, such as from cell biology or animal studies, are the primary limitations of this study. Secondly, the inherent complexity and heterogeneity of glycosylation can lead to signal dilution and complicate comprehensive quantification, as well as cause issues with ionization efficiency during mass spectrometry (MS) analysis.[42,43] Furthermore, technical biases in sample preparation, such as discrimination against certain protein types and the masking effect of highly abundant serum glycoproteins, can hinder the detection of clinically relevant glycoproteins.[44] From a translational perspective, the implementation of glycoproteomics in medical practice faces obstacles due to increased costs, technical complexity, difficulties in ensuring reproducibility, and a lack of standardization criteria, which collectively impede objective interpretation and clinical translation.[45] Lastly, study design limitations include the need for validation in larger, independent, and prospective cohorts, the importance of longitudinal studies for assessing utility in disease monitoring, and the necessity of exploring less invasive sample types (*e.g.*, blood, urine, or stool) for practical clinical application,[17] as the current study focused primarily on tissue samples.

Future directions and clinical implications

The identification of specific glycoprotein biomarkers for UC presents significant opportunities for future research and clinical application. Immediate future directions involve rigorous validation of these biomarkers in larger, diverse patient cohorts through longitudinal studies to assess their utility in tracking disease progression, response to treatment, and predicting relapse across various UC phenotypes. A crucial step for clinical translation is the development of non-invasive assays for these glycoproteins. This can be achieved using novel methods, such as enzyme-immune and protein capture biorthogonal chemistry,[46] enabling their detection in accessible biological fluids like blood, urine, or stool, and thereby reducing the need for invasive procedures. Beyond validation, integrating these glycoprotein biomarkers with other omics data (genomics, transcriptomics, metabolomics) using advanced informatics could provide a more comprehensive understanding of UC pathogenesis and lead to the discovery of more robust biomarker panels with superior predictive capabilities.[47,48] Moreover, given their functional relevance to inflammation and mucosal barrier integrity, these identified glycoproteins could also serve as novel therapeutic targets, necessitating further mechanistic studies. Ultimately, the successful translation of these glycoprotein biomarkers into clinical practice holds the potential to revolutionize UC diagnosis and management by enabling personalized medicine approaches, guiding "treat-to-target" algorithms, optimizing therapeutic efficacy, and significantly improving the quality of life for UC patients.

Conclusion

This study successfully identified three differentially expressed glycoproteins—CLCA1, FGB, and FBN1—exhibiting expression and glycosylation patterns specific to UC through a comprehensive mass spectrometry-based glycoproteomics workflow, thereby advancing the search for UC biomarkers. Complementary ELISA assays demonstrated a substantial increase of FGB and a significant decrease of CLCA1 in the serum of both UC and CD patients, while FBN1 showed no significant change in either UC or CD serum. Further studies are required to validate whether these glycoproteins are specific diagnostic markers for distinguishing between UC and CD. Subsequent GO and KEGG pathway analyses further suggested the potential functional implications of these glycoproteins in UC pathogenesis. These proteins are critically implicated in biological processes such as integrin-mediated signaling, lysosome and lytic vacuole organization, and molecular functions including endopeptidase activity, serine-type exopeptidase activity, and extracellular matrix binding. These findings collectively point to disruptions in cellular adhesion, degradation, intracellular trafficking, protein degradation, and tissue remodeling, all vital for maintaining intestinal barrier integrity. Furthermore, their association with highly significant KEGG pathways, particularly ECM-receptor interaction and complement-coagulation cascades, might correlate these glycoprotein alterations to the immune response, tissue integrity, and inflammatory processes central to UC pathogenesis. The consistent involvement of CLCA1, FGB, and FBN1, along with their altered glycosylation, in these key GO terms and pathways, strongly supports their promising potential as specific diagnostic or prognostic biomarkers for UC and/or CD, reflecting the ongoing extracellular matrix remodeling, immune dysregulation, and altered cellular degradation characteristic of the disease.

Author contributions

X. T. W., S. Y. B., and Q. K. L. conducted experiments, cultured cell lines and compiled data. Q. K. L., W. T. L., and L. J. X. collected clinical tissues. X. T. W. conducted IHC staining and ELISA. D. M. H. conceived the research. S. Y. B. conducted mass spectrometric analysis using MSFragger and Byonic. X. T. W. and S. Y. provided funding support. S. Y. conceived the work,

drafted the manuscript, and prepared all figures. All authors approved the manuscript.

Conflicts of interest

The authors declare no competing financial interests.

Data availability

This study was carried out using publicly available data from PRIDE Archive at **https://www.ebi.ac.uk/pride/archive?keyword=PXD058806&sortDirection=DESC&page=0&pageSize=20** with PXD058806.

Supplementary information: RT-qPCR method, MS data processing and protein/glycoprotein identification, statistical tests, and supplementary figures and tables. See DOI: **https://doi.org/10.1039/d5ra05241f**.

Acknowledgements

This research has received financial support from the Shantou University Medical College Start-up Fund. We extend our gratitude to the Priority Academic Program Development of the Jiangsu Higher Education Institutes (PAPD), the Jiangsu Science and Technology Plan Funding (BX2022023), the Jiangsu Shuangchuang Boshi Funding (JSSCBS20210697), the Suzhou Health Youth Talent Project (GSWS2022087), and the Suzhou Science and Technology Plan Funding (SYW2024037).

References

1 J. P. Segal, J.-F. LeBlanc and A. L. Hart, Ulcerative colitis: an update, *Clin. Med.*, 2021, **21**, 135–139.
2 M. Gajendran, P. Loganathan, G. Jimenez, A. P. Catinella, N. Ng, C. Umapathy, N. Ziade and J. G. Hashash, A comprehensive review and update on ulcerative colitis, *Disease-a-Month*, 2019, **65**, 1–37.
3 N. T. Tabarsi, N. Mortazavi, A. Norouzi, S. Besharat, N. Behnampour and N. Asgari, Association of oral manifestations with severity of the disease in ulcerative colitis patients, *BMC Gastroenterol.*, 2024, **24**, 1–7.
4 X. Wang, Y. Shen, Y. Chen and S. Yang, Inflammation-induced cellular changes: Genetic mutations, oncogene impact, and novel glycoprotein biomarkers, *Adv. Biomark. Sci. Technol.*, 2024, **6**, 91–104.
5 I. Bjarnason, The use of fecal calprotectin in inflammatory bowel disease, *Gastroenterol. Hepatol.*, 2017, **13**, 53–56.
6 S. Heinzel, J. Jureczek, V. Kainulainen, A. I. Nieminen, U. Suenkel, A.-K. von Thaler, C. Kaleta, G. W. Eschweiler, K. Brockmann, V. T. E. Aho, P. Auvinen, W. Maetzler, D. Berg and F. Scheperjans, Elevated fecal calprotectin is associated with gut microbial dysbiosis, altered serum markers and clinical outcomes in older individuals, *Sci. Rep.*, 2024, **14**, 1–13.
7 L. Newman Kira and D. R. Higgins Peter, Fecal calprotectin level is nonlinearly associated with GI pathogen detection in patients with and without inflammatory bowel disease, *J. Clin. Microbiol.*, 2023, **61**, 1–10.
8 F. S. Lehmann, F. Trapani, I. Fueglistaler, L. M. Terracciano, M. von Flüe, G. Cathomas, A. Zettl, P. Benkert, D. Oertli and C. Beglinger, Clinical and histopathological correlations of fecal calprotectin release in colorectal carcinoma, *World J. Gastroenterol.*, 2014, **20**, 4994–4999.
9 B. Singh, A. Goyal, B. C. Patel, In. *StatPearls*, eds. Singh, B., Goyal, A., Patel, B. C., StatPearls Publishing: Treasure Island (FL), 2025.
10 The Emerging Risk Factors Collaboration, C-reactive protein, fibrinogen, and cardiovascular disease prediction, *N. Engl. J. Med.*, 2012, **367**, 1310–1320.
11 S. Vermeire, G. Van Assche and P. Rutgeerts, C-reactive protein as a marker for inflammatory bowel disease, *Inflamm. Bowel Dis.*, 2004, **10**, 661–665.
12 W. D. Chey, J. Kurlander and S. Eswaran, Irritable bowel syndrome: A clinical review, *JAMA*, 2015, **313**, 949–958.
13 S. Singh, A. N. Ananthakrishnan, N. H. Nguyen, B. L. Cohen, F. S. Velayos, J. M. Weiss, S. Sultan, S. M. Siddique, J. Adler and K. A. Chachu, AGA clinical practice guideline on the role of biomarkers for the management of ulcerative colitis, *Gastroenterology*, 2023, **164**, 344–372.
14 J. Hermann, L. Schurgers and V. Jankowski, Identification and characterization of post-translational modifications: Clinical implications, *Mol. Aspects Med.*, 2022, **86**, 1–7.
15 C. Reily, T. J. Stewart, M. B. Renfrow and J. Novak, Glycosylation in health and disease, *Nat. Rev. Nephrol.*, 2019, **15**, 346–366.
16 J. Li, J. Zhang, M. Xu, Z. Yang, S. Yue, W. Zhou, C. Gui, H. Zhang, S. Li, P. G. Wang and S. Yang, Advances in glycopeptide enrichment methods for the analysis of protein glycosylation over the past decade, *J. Sep. Sci.*, 2022, **45**, 3169–3186.
17 M. Xu, A. Yang, J. Xia, J. Jiang, C.-F. Liu, Z. Ye, J. Ma and S. Yang, Protein glycosylation in urine as a biomarker of diseases, *Transl. Res.*, 2023, **253**, 95–107.
18 Z. Gao, S. Chen, J. Du, Z. Wu, W. Ge, S. Gao, Z. Zhou, X. Yang, Y. Xing, M. Shi, Y. Hu, W. Tang, J. Xia, X. Zhang, J. Jiang and S. Yang, Quantitative analysis of fucosylated glycoproteins by immobilized lectin-affinity fluorescent labeling, *RSC Adv.*, 2023, **13**, 6676–6687.
19 T. Yamada, S. Hino, H. Iijima, T. Genda, R. Aoki, R. Nagata, K.-H. Han, M. Hirota, Y. Kinashi, H. Oguchi, W. Suda, Y. Furusawa, Y. Fujimura, J. Kunisawa, M. Hattori, M. Fukushima, T. Morita and K. Hase, Mucin O-glycans facilitate symbiosynthesis to maintain gut immune homeostasis, *EBioMedicine*, 2019, **48**, 513–525.
20 A. Shubhakar, B. C. Jansen, A. T. Adams, K. R. Reiding, N. T. Ventham, R. Kalla, D. Bergemalm, P. A. Urbanowicz, R. A. Gardner, I.-B. Consortium, M. Wuhrer, J. Halfvarson, J. Satsangi, D. L. Fernandes and D. I. R. Spencer, Serum N-glycomic biomarkers predict treatment escalation in inflammatory bowel disease, *J. Crohns Colitis*, 2023, **17**, 919–932.
21 M. R. Kudelka, S. R. Stowell, R. D. Cummings and A. S. Neish, Intestinal epithelial glycosylation in

homeostasis and gut microbiota interactions in IBD, *Nat. Rev. Gastroenterol. Hepatol.*, 2020, **17**, 597–617.
22 Z. Gao, Z. Wu, Y. Han, X. Zhang, P. Hao, M. Xu, S. Huang, S. Li, J. Xia, J. Jiang and S. Yang, Aberrant fucosylation of saliva glycoprotein defining lung adenocarcinomas malignancy, *ACS Omega*, 2022, **7**, 17894–17906.
23 S. Bo, W. Xiaotong, Q. Jiani, M. Guoqiang, Y. Zheng, H. Duanmin, H. Chunyan, M. Junfeng, X. Longjiang and S. Yang, SIAE-mediated loss of sialic acid acetylation contributes to ulcerative colitis, *J. Inflamm. Res.*, 2025, **18**, 5189–5204.
24 D. B. Graham and R. J. Xavier, Pathway paradigms revealed from the genetics of inflammatory bowel disease, *Nature*, 2020, **578**, 527–539.
25 M. Schirmer, A. Garner, H. Vlamakis and R. J. Xavier, Microbial genes and pathways in inflammatory bowel disease, *Nat. Rev. Microbiol.*, 2019, **17**, 497–511.
26 A. Kaser and R. S. Blumberg, Endoplasmic reticulum stress and intestinal inflammation, *Mucosal Immunol.*, 2010, **3**, 11–16.
27 A. Kaser, E. Martínez-Naves and R. S. Blumberg, Endoplasmic reticulum stress: implications for inflammatory bowel disease pathogenesis, *Curr. Opin. Gastroenterol.*, 2010, **26**, 318–326.
28 S. Yang, W. W. Wu, R.-F. Shen, M. Bern and J. Cipollo, Identification of sialic acid linkages on intact glycopeptides via differential chemical modification using IntactGIG-HILIC, *J. Am. Soc. Mass Spectrom.*, 2018, **29**, 1273–1283.
29 S. X. Ge, D. Jung and R. Yao, ShinyGO: a graphical gene-set enrichment tool for animals and plants, *Bioinformatics*, 2020, **36**, 2628–2629.
30 E. Theodoratou, H. Campbell, N. T. Ventham, D. Kolarich, M. Pučić-Baković, V. Zoldoš, D. Fernandes, I. K. Pemberton, I. Rudan, N. A. Kennedy, M. Wuhrer, E. Nimmo, V. Annese, D. P. B. McGovern, J. Satsangi and G. Lauc, The role of glycosylation in IBD, *Nat. Rev. Gastroenterol. Hepatol.*, 2014, **11**, 588–600.
31 K. R. Jacobson, S. Lipp, A. Acuna, Y. Leng, Y. Bu and S. Calve, Comparative analysis of the extracellular matrix proteome across the myotendinous junction, *J. Proteome Res.*, 2020, **19**, 3955–3967.
32 S. Groux-Degroote, S. Cavdarli, K. Uchimura, F. Allain, and P. Delannoy, In. *Advances in Protein Chemistry and Structural Biology*, Ed. Donev, R., Academic Press, 2020, pp 111–156.
33 L. Luo, X. Wang, H. Wang, C. Yang, Y. Zhang, X. Li and Z. Xu, High cathepsin A protein expression predicts poor prognosis and tumor recurrence of hepatocellular carcinoma patients after curative hepatectomy, *Am. J. Cancer Res.*, 2022, **12**, 3843–3856.
34 H. Takeuchi, M. Schneider, D. B. Williamson, A. Ito, M. Takeuchi, P. A. Handford and R. S. Haltiwanger, Two novel protein O-glucosyltransferases that modify sites distinct from POGLUT1 and affect Notch trafficking and signaling, *Proc. Natl. Acad. Sci. U.S.A.*, 2018, **115**, E8395–E8402.
35 C. Fazio and L. Ricciardiello, Inflammation and Notch signaling: a crosstalk with opposite effects on tumorigenesis, *Cell Death Dis.*, 2016, **7**, e2515.
36 H. Lu, C. S. Fermaintt, N. A. Cherepanova, R. Gilmore, N. Yan and M. A. Lehrman, Mammalian STT3A/B oligosaccharyltransferases segregate N-glycosylation at the translocon from lipid-linked oligosaccharide hydrolysis, *Proc. Natl. Acad. Sci. U.S.A.*, 2018, **115**, 9557–9562.
37 W. Yang, P. Shah, Y. Hu, S. Toghi Eshghi, S. Sun, Y. Liu and H. Zhang, Comparison of enrichment methods for intact N- and O-linked glycopeptides using strong anion exchange and hydrophilic interaction liquid chromatography, *Anal. Chem.*, 2017, **89**, 11193–11197.
38 S. Bo, R. Zhang, L. Zhao, S. Yang, Z. Lu and P. G. Wang, High-resolution mass spectrometry for glycoproteomics, *Bioanalysis*, 2023, **15**, 57–61.
39 S. Rafique, S. Yang, M. S. Sajid and M. Faheem, A review of intact glycopeptide enrichment and glycan separation through hydrophilic interaction liquid chromatography stationary phase materials, *J. Chromatogr. A*, 2024, **1735**, 1–17.
40 R. Gulhar, M. A. Ashraf, and I. Jialal, *Physiology, Acute Phase Reactants*, StatPearls Publishing, Treasure Island (FL), 2025.
41 L. Zuliani-Alvarez and K. S. Midwood, Fibrinogen-related proteins in tissue repair: How a unique domain with a common structure controls diverse aspects of wound healing, *Adv. Wound Care*, 2014, **4**, 273–285.
42 M. Xu, H. Jin, Z. Wu, Y. Han, J. Chen, C. Mao, P. Hao, X. Zhang, C.-F. Liu and S. Yang, Mass spectrometry-based analysis of serum N-glycosylation changes in patients with Parkinson's Disease, *ACS Chem. Neurosci.*, 2022, **13**, 1719–1726.
43 J. Eichler, Protein glycosylation, *Curr. Biol.*, 2019, **29**, R229–R231.
44 S. Mehmet, G. Merve, A. Bal, K. Murat, A. Gurler and K. Elifcan, An experimental workflow for enrichment of low abundant proteins from human serum for the discovery of serum biomarkers, *JBM*, 2023, **10**, 1–11.
45 J. M. Bader, V. Albrecht and M. Mann, MS-based proteomics of body fluids: The end of the beginning, *Mol. Cell. Proteomics*, 2023, **22**, 1–18.
46 X. Wang, D. Hu, P. G. Wang and S. Yang, Bioorthogonal chemistry: Enzyme immune and protein capture for enhanced LC-MS bioanalysis, *Bioconjugate Chem.*, 2024, **35**, 1699–1710.
47 Y. Xiao, M. Bi, H. Guo and M. Li, Multi-omics approaches for biomarker discovery in early ovarian cancer diagnosis, *eBioMedicine*, 2022, **79**, 1–12.
48 R. Hussein, A. M. Abou-Shanab and E. Badr, A multi-omics approach for biomarker discovery in neuroblastoma: a network-based framework, *npj Syst. Biol. Appl.*, 2024, **10**, 1–14.